

1-1-2022

Synthesis, antioxidant activity, molecular docking and ADME studies of novel pyrrolebenzimidazole derivatives

FİKRİYE ZENGİN KARADAYI

RAHMAN BAŞARAN

MEHMET MURAT KIŞLA

BİNAY EKE

ZEYNEP ALAGÖZ

Follow this and additional works at: <https://journals.tubitak.gov.tr/chem>

 Part of the [Chemistry Commons](#)

Recommended Citation

KARADAYI, FİKRİYE ZENGİN; BAŞARAN, RAHMAN; KIŞLA, MEHMET MURAT; EKE, BİNAY; and ALAGÖZ, ZEYNEP (2022) "Synthesis, antioxidant activity, molecular docking and ADME studies of novel pyrrolebenzimidazole derivatives," *Turkish Journal of Chemistry*. Vol. 46: No. 3, Article 23. <https://doi.org/10.55730/1300-0527.3377>

Available at: <https://journals.tubitak.gov.tr/chem/vol46/iss3/23>

This Article is brought to you for free and open access by TÜBİTAK Academic Journals. It has been accepted for inclusion in Turkish Journal of Chemistry by an authorized editor of TÜBİTAK Academic Journals. For more information, please contact academic.publications@tubitak.gov.tr.

Synthesis, antioxidant activity, molecular docking and ADME studies of novel pyrrole-benzimidazole derivatives

Fikriye ZENGİN KARADAYI¹ , Rahman BAŞARAN² ,
Mehmet Murat KIŞLA¹ , Binay CAN EKE² , Zeynep ATEŞ ALAGÖZ^{1*} 

¹Department of Pharmaceutical Chemistry, Faculty of Pharmacy, Ankara University, Ankara, Turkey

²Department of Pharmaceutical Toxicology, Faculty of Pharmacy, Ankara University, Ankara, Turkey

Received: 15.02.2022 • Accepted/Published Online: 20.02.2022 • Final Version: 16.06.2022

Abstract: Several 5-(alkylsulfonyl)-1-substituted-2-(1H-pyrrol-2-yl)-1H-benzo[d]imidazole derivatives were synthesized and their antioxidant activities were investigated using lipid peroxidation (LPO) and 7-ethoxyresorufin O-deethylase (EROD) assays. Docking analysis with Human NAD[P]H-Quinone oxidoreductase 1 (NQO1) was also performed to gather thorough information about these compounds that have antioxidant activities. Moreover, their molecular descriptors and ADME properties were calculated using the SwissADME online program. As a result, most of our compounds possessed better affinity and created ample interactions with NQO1. The most potent compound **5j** had LP inhibition value of 3.73 nmol/mg/min. Other compounds exhibited moderate activity on LP levels comparing to standard butylated hydroxy toluene (**BHT**). However, the inhibitory effect on EROD activity was not significant.

Key words: Synthesis, antioxidant activity, pyrrole-benzimidazole, molecular docking, lipid peroxidation

1. Introduction

Antioxidant defense mechanisms, including enzymatic and nonenzymatic systems, play a key role in cellular physiology and survival maintenance by preventing oxidative stress-related cellular damage [1,2]. The imbalance between oxygen-derived free radicals and antioxidant defense systems can lead to this damage by disrupting these antioxidant mechanisms. Eventual antioxidant capacity deficiency can be treated with novel compounds with antioxidant activity and free radical scavenging properties. Lipid peroxidation (LPO), which is one of the most commonly used assays to analyze in vitro antioxidant activity of a new compound, is an oxidative process mediated by reactive oxygen species (ROS) that results in damage to cellular membranes and other lipid-containing structures [3]. ROS can be generated by CYP450 enzymes while they are catalyzing their endogenous and exogenous substrates, and in the end, ROS would lead to the generation of potentially carcinogenic and mutagenic lipid peroxidation (LPO) end products. Among CYP450 enzyme family, CYP1A1 is of great importance in NADPH-dependent LPO. Therefore, probing the effects of antioxidant drug candidates on the catalytic activity of CYP450 enzymes and LPO levels is crucial. [4].

In NADPH-dependent LPO, NAD(P)H:quinone acceptor oxidoreductases (NQO's) are flavoenzymes that effectively catalyze the reduction of quinone derivatives to hydroquinones [5]. The quinones are electrophilic molecules that can alkylate certain biopolymers such as proteins and DNA in cells. Reduction of quinones with one electron generates the semiquinone radicals and ROS that can induce cellular damage. NQO1, a major member of the NAD(P)H:quinone acceptor oxidoreductases family, contains flavin adenine dinucleotide (FAD) for its stability and proper function and is also highly inducible under oxidative stress. This enzyme can assist the protection of antioxidant substances such as ubiquinone, α -tocopherol quinone, PARP (Poly (ADP-ribose) polymerase) as well as its macromolecular binding functions and may contribute to the cellular protective response. Considering this knowledge about NQO1, a docking analysis has been conducted to identify whether our compounds interact with this enzyme in a similar manner to the literature [6].

Pyrroles and benzimidazole ring systems exhibit various biological activities including antioxidant, antibacterial, and anticancer properties [7–12]. The effects of the benzimidazole ring on the CYP system have been known for a long time. The ability of imidazole derivatives to inhibit some CYP activities has been studied. These studies have shown that the ability of compounds to interact with CYPs is largely dependent on their lipophilic and electronic characters

* Correspondence: zates@pharmacy.ankara.edu.tr

[13–16]. In our previous papers, we applied the strategy of using particular benzimidazole conjugates as antioxidant agents [1,17,18]. In light of data obtained from our previous studies, we still explore the potential new benzimidazole derivatives with strong antioxidant activities. For instance, we have synthesized and characterized some new 6-fluoro-5-substituted-benzimidazole compounds bearing an indole ring at the second position of the benzimidazole ring and then evaluated their antioxidant capacities *in vitro*. At the 10^{-3} M concentrations, almost all the synthesized compounds exhibited remarkable superoxide anion formation inhibitory effects compared to that of superoxide dismutase [19]. In this study, we have aimed to conjugate pyrrole fragments instead of an indole ring to the benzimidazole from the second position to evaluate their antioxidant activities and structure-activity relationships. Herein, some new 5-(alkylsulfonyl)-1-substituted-2-(1H-pyrrol-2-yl)-1H-benzo[d]imidazole derivatives (**5a-n**) were designed, synthesized, characterized, and were analyzed *in silico* and *in vitro*. Their free radical scavenging properties were then probed *in vitro* by employing lipid peroxidation (LPO) and 7-ethoxyresorufin O-deethylase (EROD) assays to verify their potential antioxidant activities and structure-activity relationship.

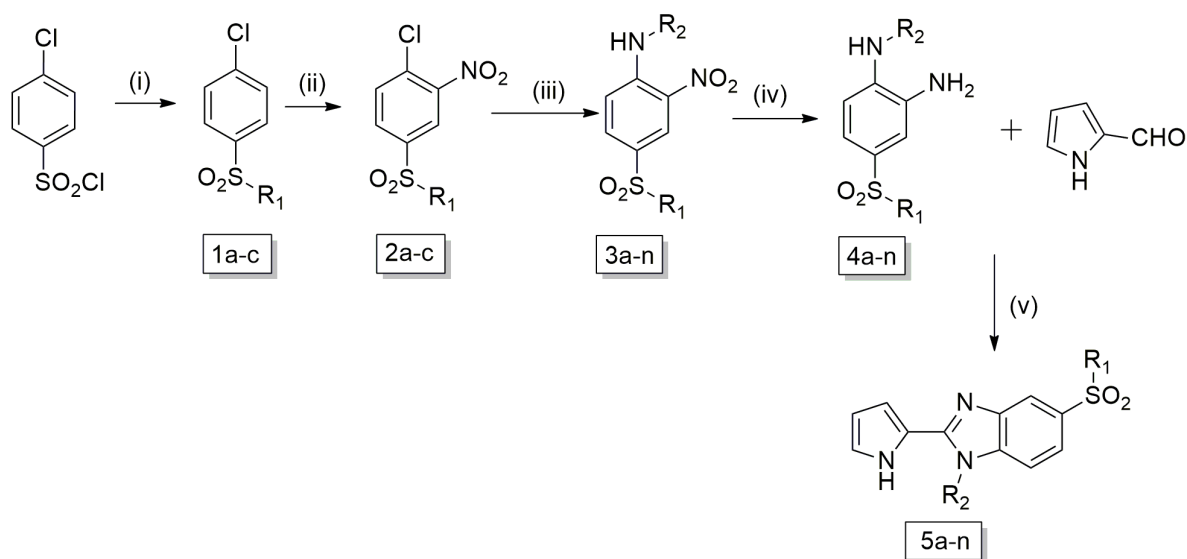
2. Materials and methods

2.1. Chemistry

Büchi SMP-20 (Büchi Labortechnik, Flawil, Switzerland) and Electrothermal 9100 capillary melting point apparatus (Electrothermal, Essex, UK) were used for determination and uncorrection of the melting points. Varian Mercury-400 FT-NMR spectrometer (Varian Inc., Palo Alto, CA, USA) was used for recording the ^1H NMR and ^{13}C NMR spectra, and LC-MS spectrometer (Waters Corporation, Milford, MA, USA) was used to record the Mass spectra based on ESI(+). LECO 932 CHNS (Leco - 932, St. Joseph, MI, USA) instrument was used for elemental analysis. For column chromatography (cc), silica gel 60 (40–63 mm particle size) was used. 4-Chlorobenzenesulfonylchloride, 1-chloro-4-(methylsulfonyl) benzene (**1a**), and pyrrole-2-carboxaldehyde are commercially available and purchased from Sigma-Aldrich company. Synthesis of new compounds **5a-n** outlined in Figure 1. 4-chloro-benzenesulfonyl chloride was used as starting material (**1**). Compounds **1b**, **1c**, and **2a-c** were prepared according to the previous publications [20–24].

2.1.1. General procedure for synthesis of **3a-n**

To the solution of 4-(alkylsulfonyl)-1-chloro-2-nitrobenzene (**2a-c**) (5 mmol) in ethanol (5 mL), amine derivative (15 mmol) was added and heated under reflux, until the starting material was consumed (determined by TLC, 8–48 h). Upon cooling the mixture, water was added. The resultant yellow residue was crystallized from ethanol or purified by cc by using a mixture of hexane and ethyl acetate in varying concentrations as eluent [20].



(i) Te-Rongalite, 1 M NaOH, R_1 , THF (90°C, 5 h); (ii) KNO_3 , H_2SO_4 , 90°C, 2 h; (iii) R_2NH_2 , EtOH, reflux, 8–48 h; (iv) H_2 , Pd/C, EtOH; (v) $\text{Na}_2\text{S}_2\text{O}_5$, EtOH, reflux (4–12 h).

Figure 1. Synthesis procedure of novel pyrrole-benzimidazole derivatives **5a-n**.

2.1.2. General procedure for synthesis of 4a-n

Compounds **3a-n** (3.5 mmol) in EtOH (75 mL) reduced by hydrogenation using 40 psi of H₂ and 10% Pd/C (40 mg) until cessation of H₂ uptake to obtain the catalyst before filtering off on a bed of celite and washing with EtOH; and concentrating the filtrate in vacuo [22]. The crude amine was used without purification [23].

2.1.3. General procedure for synthesis of 5a-n

A mixture of the appropriate *o*-phenylenediamine (**4a-n**, 1 mmol), pyrrole-2-carboxaldehyde (1 mmol) and Na₂S₂O₅ (40%) (2 mL) in EtOH (4 mL), was refluxed until the starting material was consumed (determined by TLC, 4–12 h). The reaction mixture was poured into water, and the precipitate was filtered and washed with water. The residue was purified by cc to give the final product (**5a-n**) (Figure 1) [19,23].

2.1.3.1. 1-Methyl-5-(methylsulfonyl)-2-(1*H*-pyrrol-2-yl)-1*H*-benzo[*d*]imidazole (5a)

Compound **5a** was prepared according to general methods starting from *N*¹-(methyl)-4-(methylsulfonyl)benzene-1,2-diamine (1.81 mmol, 0.363 g) and pyrrol-3-carboxaldehyde (1.81 mmol, 0.172 g). The residue was purified by cc using the mixture of chloroform - ethyl acetate - hexane (2:2:1) as eluent to give a white solid, m.p. 259 °C (0.045 g, 10% yield). ¹H NMR (400 MHz, DMSO - *d*6): δ ppm 3.23 (s, 3H), 4.02 (s, 3H), 6.30–6.32 (m, 1H), 6.94 (t, 1H), 7.07 (d, *J* = 1.2 Hz, 1H), 7.76 (dd, *J* = 1.6 Hz, *J* = 8.4 Hz, 1H), 7.84 (d, *J* = 8.8 Hz, 1H), 8.07 (d, *J* = 1.6 Hz, 1H), 11.99 (s, 1H). ¹³C NMR (DMSO - *d*6) δ ppm 31.9, 44.2, 109.7, 110.7, 117.0, 120.0, 120.3, 122.5, 134.2, 139.5, 141.8, 149.9. MS (ESI +) *m/z*: 276. Anal. calcd. for C₁₃H₁₃N₃O₂S-0.15 H₂O: C, 56.15; H, 4.82; N, 15.11; S, 11.53; Found: C, 56.02; H, 4.72; N, 15.10; S, 11.48.

2.1.3.2. 1-Ethyl-5-(methylsulfonyl)-2-(1*H*-pyrrol-2-yl)-1*H*-benzo[*d*]imidazole (5b)

Compound **5b** was prepared according to general methods starting from *N*¹-(ethyl)-4-(methylsulfonyl)benzene-1,2-diamine (1.03 mmol, 0.222 g) and pyrrol-3-carboxaldehyde (1.03 mmol, 0.097 g). The residue was purified by cc using the mixture of chloroform - ethyl acetate - hexane (2:2:1) as eluent to give a white solid, m.p. 204 °C (0.171 g, 57% yield). ¹H NMR (400 MHz, DMSO - *d*6): δ ppm 1.40 (t, 3H), 3.23 (s, 3H), 4.54 (q, 2H), 6.31–6.33 (m, 1H), 6.85–6.87 (m, 1H), 7.06–7.07 (m, 1H), 7.77 (dd, *J* = 1.6 Hz, *J* = 8.4 Hz, 1H), 7.86 (d, *J* = 8.4 Hz, 1H), 8.09 (d, *J* = 1.6 Hz, 1H), 11.95 (s, 1H). ¹³C NMR (DMSO - *d*6) δ ppm 14.5, 44.2, 48.6, 109.9, 110.6, 110.7, 120.0, 120.2, 122.5, 134.4, 138.6, 142.0, 149.0. MS (ESI +) *m/z*: 290. Anal. calcd. for C₁₄H₁₅N₃O₂S - 0.3 H₂O: C, 57.04; H, 5.33; N, 14.25; S, 10.87; Found: C, 56.93; H, 5.35; N, 14.35; S, 11.02.

2.1.3.3. 1-propyl-5-(methylsulfonyl)-2-(1*H*-pyrrol-2-yl)-1*H*-benzo[*d*]imidazole (5c)

Compound **5c** was prepared according to general methods starting from *N*¹-(propyl)-4-(methylsulfonyl)benzene-1,2-diamine (0.76 mmol, 0.174 g) and pyrrol-3-carboxaldehyde (0.76 mmol, 0.073 g). The residue was purified by cc using the mixture of chloroform - ethyl acetate - hexane (1:2:1) as eluent to give a white solid, m.p. 189 °C (0.053 g, 23% yield). ¹H NMR (400 MHz, DMSO - *d*6): δ ppm 0.94 (t, 3H), 1.82 (m, 2H), 3.24 (s, 3H), 4.46 (t, 2H), 6.30–6.32 (m, 1H), 6.82 (s, 1H), 7.06 (d, *J* = 0.8 Hz, 1H), 7.76 (dd, *J* = 1.6 Hz, *J* = 8.2 Hz, 1H), 7.87 (d, *J* = 8.8 Hz, 1H), 8.08 (d, *J* = 1.2 Hz, 1H), 11.95 (s, 1H). ¹³C NMR (DMSO - *d*6) δ ppm 10.8, 22.3, 44.2, 45.4, 109.9, 110.6, 110.9, 117.1, 120.1, 120.1, 122.4, 134.3, 139.1, 141.8, 149.2. MS (ESI +) *m/z*: 304. Anal. calcd. for C₁₅H₁₇N₃O₂S - 0.2 H₂O: C, 58.68; H, 5.71; N, 13.68; S, 10.44; Found: C, 58.36; H, 5.67; N, 13.69; S, 10.41.

2.1.3.4. 1-Butyl-5-(methylsulfonyl)-2-(1*H*-pyrrol-2-yl)-1*H*-benzo[*d*]imidazole (5d)

Compound **5d** was prepared according to general methods starting from *N*¹-(butyl)-4-(methylsulfonyl)benzene-1,2-diamine (0.70 mmol, 0.171 g) and pyrrol-3-carboxaldehyde (0.70 mmol, 0.067 g). The residue was purified by cc using the mixture of chloroform - ethyl acetate - hexane (2:3:3) as eluent to give a white solid, m.p. 151 °C (0.098 g, 44% yield). ¹H NMR (400 MHz, DMSO - *d*6): δ ppm 0.87 (t, 3H), 1.34 (m, 2H), 1.74 (m, 2H), 3.21 (s, 3H), 4.47 (t, 2H), 6.27–6.29 (m, 1H), 6.80 (s, 1H), 7.03 (d, *J* = 1.2 Hz, 1H), 7.74 (dd, *J* = 1.6 Hz, *J* = 8.8 Hz, 1H), 7.83 (d, *J* = 8.8 Hz, 1H), 8.05 (d, *J* = 1.6 Hz, 1H), 11.92 (s, 1H). ¹³C NMR (DMSO - *d*6) δ ppm 13.5, 19.3, 31.0, 43.9, 44.1, 109.8, 110.6, 110.8, 117.0, 120.0, 120.1, 122.3, 134.2, 139.0, 141.7, 149.1. MS (ESI +) *m/z*: 318. Anal. calcd. for C₁₆H₁₉N₃O₂S: C, 60.20; H, 6.06; N, 13.16; S, 10.04; Found: C, 60.18; H, 6.09; N, 13.29; S, 10.15.

2.1.3.5. 1-Cyclohexyl-5-(methylsulfonyl)-2-(1*H*-pyrrol-2-yl)-1*H*-benzo[*d*]imidazole (5e)

Compound **5e** was prepared according to general methods starting from *N*¹-(cyclohexyl)-4-(methylsulfonyl)benzene-1,2-diamine (1.00 mmol, 0.27 g) and pyrrol-3-carboxaldehyde (1.00 mmol, 0.096 g). The residue was purified by cc using the mixture of chloroform - ethyl acetate - hexane (1:1.5:0.5) as eluent to give a white solid, m.p. 252 °C (0.138 g, 40% yield). ¹H NMR (400 MHz, DMSO - *d*6): δ ppm 1.42–1.44 (m, 3H), 1.69 (s, 1H), 1.88–1.96 (m, 4H), 2.26–2.34 (m, 2H), 3.21 (s, 3H), 4.74–4.80 (m, 1H), 6.29 (d, *J* = 1.6 Hz, 1H), 6.60 (t, 1H), 7.04 (s, 1H), 7.68 (dd, *J* = 1.6 Hz, *J* = 8.6 Hz, 1H), 8.05 (s, 1H), 8.07 (d, *J* = 1.6 Hz, 1H), 11.88 (s, 1H). ¹³C NMR (DMSO - *d*6) δ ppm 24.3, 25.4, 30.3, 44.1, 56.6, 109.5, 110.7, 113.4, 117.6, 119.7, 119.8, 122.0, 134.0, 136.9, 142.7, 149.6. MS (ESI +) *m/z*: 344. Anal. calcd. for C₁₈H₂₁N₃O₂S - 0.3H₂O: C, 61.97; H, 6.24; N, 12.04; S, 9.19; Found: C, 61.96; H, 6.15; N, 12.13; S, 9.23.

2.1.3.6. 1-Benzyl-5-(methylsulfonyl)-2-(1H-pyrrol-2-yl)-1H-benzo[d]imidazole (5f)

Compound **5f** was prepared according to general methods starting from *N*¹-(benzyl)-4-(methylsulfonyl)benzene-1,2-diamine (0.70 mmol, 0.188 g) and pyrrol-3-carboxaldehyde (0.70 mmol, 0.067 g). The residue was purified by cc using the mixture of chloroform - ethyl acetate - hexane (2:3:3) as eluent to give a white solid, m.p. 172 °C (0.096 g, 39% yield). ¹H NMR (400 MHz, DMSO - *d*6): δ ppm 3.24 (s, 3H), 5.81 (s, 2H), 6.19 (s, 1H), 6.59 (t, 1H), 7.03 (s, 1H), 7.08 (d, *J* = 7.2 Hz, 2H), 7.27-7.35 (m, 3H), 7.59–7.76 (m, 2H), 8.14 (s, 1H), 12.01 (s, 1H). ¹³C NMR (DMSO - *d*6) δ ppm 44.1, 47.3, 109.8, 110.9, 111.1, 117.2, 119.8, 120.5, 122.6, 125.9, 127.4, 128.8, 134.7, 136.3, 139.4, 142.0, 149.7. MS (ESI +) *m/z*: 352. Anal. calcd. for C₁₉H₁₇N₃O₂S - 0.4 H₂O: C, 63.63; H, 5.00; N, 11.71; S, 8.94; Found: C, 63.24; H, 4.86; N, 11.64; S, 8.87.

2.1.3.7. 1-(4-Fluorobenzyl)-5-(methylsulfonyl)-2-(1H-pyrrol-2-yl)-1H-benzo[d]imidazole (5g)

Compound **5g** was prepared according to general methods starting from *N*¹-(4-fluorobenzyl)-4-(methylsulfonyl)benzene-1,2-diamine (0.94 mmol, 0.277 g) and pyrrol-3-carboxaldehyde (0.94 mmol, 0.089 g). The residue was purified by cc using the mixture of chloroform - ethyl acetate - hexane (2:3:3) as eluent to give a white solid, m.p. 162 °C (0.051 g, 15% yield). ¹H NMR (400 MHz, DMSO - *d*6): δ ppm 3.22 (s, 3H), 5.77 (s, 2H), 6.18 (s, 1H), 6.59 (s, 1H), 7.01 (s, 1H), 7.08–7.17 (m, 4H), 7.72–7.77 (m, 2H), 8.11 (1H), 11.99 (s, 1H). ¹³C NMR (DMSO - *d*6) δ ppm 44.1, 46.7, 109.8, 110.9, 110.1, 115.7 (d, *J* = 21.4 Hz), 117.3, 119.6, 122.7, 128.07 (d, *J* = 7.6 Hz), 132.5 (d, *J* = 3.1 Hz), 134.8, 139.2, 142.6, 161.3 (d, *J* = 242.3 Hz). MS (ESI+) *m/z*: 370. Anal. calcd. for C₁₉H₁₆FN₃O₂S - 0.45 H₂O: C, 60.44; H, 4.51; N, 11.13; S, 8.49; Found: C, 60.18; H, 4.36; N, 11.06; S, 8.60.

2.1.3.8. 1-(4-Chlorobenzyl)-5-(methylsulfonyl)-2-(1H-pyrrol-2-yl)-1H-benzo[d]imidazole (5h)

Compound **5h** was prepared according to general methods starting from *N*¹-(4-chlorobenzyl)-4-(methylsulfonyl)benzene-1,2-diamine (0.78 mmol, 0.243 g) and pyrrol-3-carboxaldehyde (0.78 mmol, 0.075 g). The residue was purified by cc using the mixture of chloroform - ethyl acetate - hexane (2:3:3) as eluent to give a white solid, m.p. 193 °C (0.113 g, 37% yield). ¹H NMR (400 MHz, DMSO - *d*6): δ ppm 3.25 (s, 3H), 5.81 (s, 2H), 6.19 - 6.21 (m, 1H), 6.57–6.59 (m, 1H), 7.03–7.04 (m, 1H), 7.10 (d, *J* = 8.0 Hz, 2H), 7.38–7.42 (m, 2H), 7.76–7.77 (m, 2H), 8.14 (d, *J* = 0.8 Hz, 1H), 12.02 (s, 1H). ¹³C NMR (DMSO - *d*6) δ ppm 44.1, 46.7, 109.8, 110.9, 111.1, 117.3, 119.7, 120.6, 122.7, 127.8, 128.8, 132.0, 134.8, 135.4, 139.2, 142.0, 149.6. MS (ESI +) *m/z*: 386. Anal. calcd. for C₁₉H₁₆ClN₃O₂S - 0.1 H₂O: C, 58.86; H, 4.21; N, 10.83; S, 8.27; Found: C, 58.74; H, 4.19; N, 10.85; S, 8.26.

2.1.3.9. 1-Propyl-5-(ethylsulfonyl)-2-(1H-pyrrol-2-yl)-1H-benzo[d]imidazole (5i)

Compound **5i** was prepared according to general methods starting from *N*¹-(propyl)-4-(ethylsulfonyl)benzene-1,2-diamine (0.88 mmol, 0.215 g) and pyrrol-3-carboxaldehyde (0.88 mmol, 0.085 g). The residue was purified by cc using the mixture of chloroform - ethyl acetate - hexane (2:1:1) as eluent to give a white solid, m.p. 146 °C (0.046 g, 16% yield). ¹H NMR (400 MHz, DMSO - *d*6): δ ppm 0.94 (t, 3H), 1.12 (t, 3H), 1.80–1.85 (m, 2H), 3.31 (q, 2H), 4.46 (t, 2H), 6.31 (m, 1H), 6.82 (s, 1H), 7.06 (d, *J* = 0.8 Hz, 1H), 7.71 (dd, *J* = 1.6 Hz, *J* = 9.0 Hz, 1H), 7.88 (d, *J* = 8.8 Hz, 1H), 8.03 (d, *J* = 1.6 Hz, 1H), 11.95 (s, 1H). ¹³C NMR (DMSO - *d*6) δ ppm 7.3, 10.8, 22.3, 45.5, 49.7, 109.9, 110.7, 110.9, 117.9, 120.1, 120.9, 122.4, 131.8, 139.3, 141.9, 149.2. MS (ESI +) *m/z*: 318. Anal. calcd. for C₁₆H₁₉N₃O₂S: C, 60.54; H, 6.03; N, 13.23; S, 10.10; Found: C, 60.68; H, 6.23; N, 13.14; S, 10.07.

2.1.3.10. 1-Benzyl-5-(ethylsulfonyl)-2-(1H-pyrrol-2-yl)-1H-benzo[d]imidazole (5j)

Compound **5j** was prepared according to general methods starting from *N*¹-(benzyl)-4-(ethylsulfonyl)benzene-1,2-diamine (0.95 mmol, 0.277 g) and pyrrol-3-carboxaldehyde (0.95 mmol, 0.091 g). The residue was purified by cc using the mixture of chloroform - ethyl acetate - hexane (2:1:1) as eluent to give a white solid, m.p. 183 °C (0.130 g, 38% yield). ¹H NMR (400 MHz, DMSO - *d*6): δ ppm 1.10 (t, 3H), 3.29 (q, 2H), 5.78 (s, 2H), 6.15–6.18 (m, 1H), 6.56 (s, 1H), 7.01 (s, 1H), 7.06 (d, *J* = 8.4 Hz, 2H), 7.24 (d, *J* = 8.4 Hz, 1H), 7.30 (t, 2H), 7.69 (dd, *J* = 1.2 Hz, *J* = 8. Hz, 1H), 7.75 (d, *J* = 8.0 Hz, 1H), 8.07 (d, *J* = 1.2 Hz, 1H), 12.00 (s, 1H). ¹³C NMR (DMSO - *d*6) δ ppm 7.3, 47.3, 49.6, 109.8, 111.0, 111.1, 118.1, 119.8, 121.3, 122.7, 125.9, 127.5, 128.9, 132.2, 136.4, 139.5, 142.0, 149.7. MS (ESI +) *m/z*: 366. Anal. calcd. for C₂₀H₁₉N₃O₂S: C, 65.73; H, 5.24; N, 11.50; S, 8.77; Found: C, 65.81; H, 5.39; N, 11.26; S, 8.68.

2.1.3.11. 1-(4-Fluorobenzyl)-5-(ethylsulfonyl)-2-(1H-pyrrol-2-yl)-1H-benzo[d]imidazole (5k)

Compound **5k** was prepared according to general methods starting from *N*¹-(p-fluorobenzyl)-4-(ethylsulfonyl)benzene-1,2-diamine (0.62 mmol, 0.193 g) and pyrrol-3-carboxaldehyde (0.62 mmol, 0.060 g). The residue was purified by cc using the mixture of chloroform - ethyl acetate - hexane (2:1:1) as eluent to give a white solid, m.p. 164 °C (0.058 g, 24% yield). ¹H NMR (400 MHz, DMSO - *d*6): δ ppm 1.12 (t, 3H), 3.31 (q, 2H), 5.79 (s, 2H), 6.20 (q, 1H), 6.61 (s, 1H), 7.03–7.04 (m, 1H), 7.11–7.19 (m, 4H), 7.70 (dd, *J* = 1.6 Hz, *J* = 8.4 Hz, 1H), 7.79 (d, *J* = 8.8 Hz, 1H), 8.08 (d, *J* = 1.2 Hz, 1H), 12.00 (s, 1H). MS (ESI +) *m/z*: 384. Anal. calcd. for C₂₀H₁₈FN₃O₂S - 0.1H₂O: C, 62.35; H, 4.76; N, 10.90; S, 8.32; Found: C, 62.16; H, 4.98; N, 10.77; S, 8.20.

2.1.3.12. 1-(3,4-Difluorobenzyl)-5-(ethylsulfonyl)-2-(1H-pyrrol-2-yl)-1H-benzo[d]imidazole (5l)

Compound **5l** was prepared according to general methods starting from *N*¹-(3,4-difluorobenzyl)-4-(ethylsulfonyl) benzene-1,2-diamine (0.77 mmol, 0.254 g) and pyrrol-3-carboxaldehyde (0.77 mmol, 0.074 g). The residue was purified by cc using the mixture of chloroform - ethyl acetate - hexane (2:2:1) as eluent to give a white solid, m.p. 182 °C (0.112 g, 36% yield). ¹H NMR (400 MHz, DMSO - *d*6): δ ppm 1.13 (t, 3H), 3.32 (q, 2H), 5.81 (s, 2H), 6.22 (q, 1H), 6.62 (s, 1H), 6.82 (d, *J* = 8.0 Hz, 1H), 7.06 (d, *J* = 0.8 Hz, 1H), 7.26–7.42 (m, 2H), 7.72 (dd, *J* = 1.6 Hz, *J* = 8.4 Hz, 1H), 7.81 (d, *J* = 8.4 Hz, 1H), 8.10 (d, *J* = 1.6 Hz, 1H), 12.03 (s, 1H). ¹³C NMR (DMSO - *d*6) δ ppm 7.2, 46.3, 49.6, 109.8, 110.8, 111.0, 115.4, 115.6, 117.9, 118.0, 118.1, 119.6, 121.3, 122.7, 132.4, 139.2, 142.05, 149.5, 149.7. MS (ESI+) *m/z*: 402. Anal. calcd. for C₂₀H₁₇F₂N₃O₂S: C, 59.83; H, 4.26; N, 10.46; S, 7.98; Found: C, 59.60; H, 4.28; N, 10.42; S, 8.02.

2.1.3.13. 1-(3,4-Dichlorobenzyl)-5-(ethylsulfonyl)-2-(1H-pyrrol-2-yl)-1H-benzo[d]imidazole (5m)

Compound **5m** was prepared according to general methods starting from *N*¹-(3,4-dichlorobenzyl)-4-(ethylsulfonyl) benzene-1,2-diamine (0.62 mmol, 0.225 g) and pyrrol-3-carboxaldehyde (0.62 mmol, 0.059 g). The residue was purified by cc using the mixture of chloroform - ethyl acetate - hexane (2:2:1) as eluent to give a white solid, m.p. 191 °C (0.062 g, 23% yield). ¹H NMR (400 MHz, DMSO - *d*6): δ ppm 1.12 (t, 3H), 3.32 (q, 2H), 5.83 (s, 2H), 6.21 (q, 1H), 6.60 (s, 1H), 6.93 (dd, *J* = 1.6 Hz, *J* = 8.6 Hz, 1H), 7.05 (s, 1H), 7.47 (d, *J* = 1.6 Hz, 1H), 7.57 (d, *J* = 8.8 Hz, 1H), 7.7 (dd, *J* = 1.6 Hz, *J* = 8.8 Hz, 1H), 7.80 (d, *J* = 8.0 Hz, 1H), 8.09 (d, *J* = 1.2 Hz, 1H), 12.03 (s, 1H). ¹³C NMR (DMSO - *d*6) δ ppm 7.3, 46.3, 49.6, 109.9, 110.9, 111.1, 118.2, 119.6, 121.5, 122.9, 126.1, 128.3, 130.1, 131.1, 131.4, 132.5, 137.6, 139.3, 142.1, 149.6. MS (ESI+) *m/z*: 435. Anal. calcd. for C₂₀H₁₇Cl₂N₃O₂S: C, 55.30; H, 3.94; N, 9.67; S, 7.38; Found: C, 55.33; H, 3.94; N, 9.78; S, 7.39.

2.1.3.14. 1-(3,4-Dichlorobenzyl)-5-(propylsulfonyl)-2-(1H-pyrrol-2-yl)-1H-benzo[d]imidazole (5n)

Compound **5n** was prepared according to general methods starting from *N*¹-(3,4-dichlorobenzyl)-4-(propylsulfonyl) benzene-1,2-diamine (0.61 mmol, 0.228 g) and pyrrol-3-carboxaldehyde (0.61 mmol, 0.058 g). The residue was purified by cc using the mixture of chloroform - ethyl acetate - hexane (2:3:3) as eluent to give a white solid, m.p. 196 °C (0.075 g, 27% yield). ¹H NMR (400 MHz, DMSO - *d*6): δ ppm 0.91 (t, 3H), 1.55 - 1.61 (m, 2H), 3.30 (t, 2H), 5.82 (s, 2H), 6.20–6.22 (m, 1H), 6.59 (s, 1H), 6.92 (dd, *J* = 2.0 Hz, *J* = 9.0 Hz, 1H), 7.04–7.05 (m, 1H), 7.46 (d, *J* = 2.0 Hz, 1H), 7.57 (d, *J* = 8.0 Hz, 1H), 7.71 (dd, *J* = 2.0 Hz, *J* = 9.0 Hz, 1H), 7.80 (d, *J* = 8.8 Hz, 1H), 8.08 (d, *J* = 1.6 Hz, 1H), 12.03 (s, 1H). ¹³C NMR (DMSO - *d*6) δ 12.5, 16.3, 46.3, 56.7, 109.9, 110.8, 111.1, 118.0, 119.6, 121.3, 122.8, 126.1, 128.3, 130.1, 131.1, 131.4, 133.1, 137.6, 139.3, 142.0, 149.5. MS (ESI+) *m/z*: 449. Anal. calcd. for C₂₁H₁₉Cl₂N₃O₂S: C, 56.25; H, 4.27; N, 9.37; S, 7.15; Found: C, 55.96; H, 4.25; N, 9.46; S, 7.19.

2.2. In vitro antioxidant activity**2.2.1. Treatment of animals**

Albino male Wistar rats with 200–225 g were used in the present study. They were individually housed in standard cages with free access to tap water and standard rat chow ad libitum and maintained at room temperature of 22–25 °C, a 12 h light-dark cycle, and 60% relative humidity. Rats were deprived of feed for 24 h before decapitation under anaesthesia. The liver tissues were dissected quickly, rinsed thoroughly with deionized water, weighed, and then immediately stored at –80 °C to minimize any potential changes before processing. All housing and experimental procedures were approved by Ankara University Animal Ethics Committee.

2.2.2. Isolation of rat liver microsomes

Rat liver tissues were homogenized in cold 1.15% KCl (w/v) with a homogenizer on ice at 250 x g. The homogenates were first centrifuged at 11,000 x g for 25 min at 4 °C and the resulting supernatants were collected and further ultracentrifuged at 108,000 x g for 60 min at 4 °C. The latter pellets were suspended with 20% glycerol and maintained at –80 °C until further analysis. Total microsomal protein concentrations were quantified by the protocol of Lowry et al. [25], using bovine serum albumin as a standard.

2.2.3. Lipid peroxidation (LPO) assay

Lipid peroxidation (LPO) level was determined based on the protocols reported by Wills [26,27], and Bishayee and Balasubramanian [28], with some modifications described previously [29]. The assay employs the measurement of thiobarbituric acid reactive substances (TBARS) that yields a pink color and can be measured spectrophotometrically at 532 nm, resulting from the reaction between lipid peroxidation products, mainly malondialdehyde (MDA), and thiobarbituric acid (TBA) under acidic conditions and high temperature. The final reaction mixture (1 mL) in the test tube consists of 0.2 mg microsomal protein, 10⁻³ M test compound, 62.5 mM potassium phosphate buffer (pH: 7.4), 90 mM KCl, 0.2 mM Fe²⁺, in which cofactor (NADPH - generating system containing of 2.5 mM MgCl₂, 0.25 mM NADP⁺, 2.5 mM glucose-6-phosphate, 14.2 mM potassium phosphate buffer (pH 7.8), and 1.0 U glucose-6-phosphate dehydrogenase) was added to initiate the reaction. Next, the mixture was incubated at 37 °C in a shaking water bath. After 30 min of incubation,

the reaction was terminated by the addition of 500 μL of 25 % (w/v) trichloroacetic acid (TCA) and the mixture was then centrifuged at 7000 x g for 20 min to remove denatured proteins. One milliliter of the supernatant was mixed with 0.5 mL of TBA and then heated for 20 min in a boiling water bath. The absorbance of TBARS was measured at 532 nm against the blank, which contains all reagents without microsomal proteins. The results were then expressed as nmol TBARS/mg of protein. In this protocol, while dimethyl sulfoxide (DMSO), in which the synthesized compounds were dissolved, was employed as the control, butylated hydroxyl toluene (BHT) was used as a standard.

2.2.4. 7-Ethoxyresorufin O-deethylase (EROD) assay

7-Ethoxyresorufin O-deethylase (EROD) activity was assayed by the protocol described by Burke et al. [30]. EROD activity is measured by following the CYP1A1-mediated deethylation of the substrate 7-ethoxyresorufin to form the product resorufin that can be monitored fluorometrically [30]. The final reaction mixture (1 mL) in the test tube consists of 0.2 mg microsomal protein, 10^{-3} M test compound, 1.0 mM 7-ethoxyresorufin as a substrate, 12 mM albumin, 100 mM Tris - HCl buffer (pH 7.8), in which cofactor (NADPH - generating system consisting of 0.25 mM NADP⁺, 2.5 mM MgCl₂, 2.5 mM glucose-6-phosphate, 14.2 mM potassium phosphate buffer (pH 7.8), and 1.0 U glucose-6-phosphate dehydrogenase) was added to initiate the reaction. Next, the mixture was incubated at 37 °C for 5 min in a shaking water bath. After incubation, the reaction was terminated by the addition of 3 mL ice cold methanol and the mixture was then centrifuged at 7 000 x g for 20 min to remove denatured proteins. Following the centrifugation, the fluorescence intensity of the supernatant (3 mL) was read at the excitation/emission wavelengths of 538 nm/587 nm. While caffeine was employed as a standard, the control used in this protocol was dimethyl sulfoxide (DMSO) in which the synthesized compounds were dissolved.

2.2.5. Docking method and ADME property calculation

Human NAD[P]H-Quinone oxidoreductase 1 (PDB ID : 1dxo, resolution: 2.5 Å) file was obtained from the RCSB Protein Data Bank website [31]. AutoDockTools v.1.5.6 was used for deleting water molecules and defining the grid box [32]. Following this process, polar hydrogens and Gasteiger charges were added, and the grid was also prepared using the same software. Assigned grid's center were X = -2.718, Y = 16.674, Z = 5.139 and dimensions were X = 40, Y = 40, Z = 40. Spacing was defined as 0.375 Å. The 2D structures of the compounds were drawn on ChemDraw Ultra 12.0, minimized with MMFF94 and UFF force fields (number of steps: 5000 with steepest descent algorithm and convergence value of $10e-7$) and then these files were converted to pdb files using Avogadro software [33]. Subsequently, Gasteiger charges and torsion were added to ligand files with AutoDockTools. Prepared ligands were docked with AutoDock Vina [34]. Finally, 3-D docked poses and interaction diagrams of the ligands were generated and interpreted using Discovery Studio Visualizer Ligand interaction module [35].

The evaluation of physicochemical properties and the prediction of ADME parameters were determined with SwissADME online tools [36]. Besides, using BOILED-Egg representation brain penetration and gastrointestinal absorption of synthesized compounds were assessed [37]. With the aid of the abovementioned calculations, we aimed to gather medicinal chemistry information about our compound set and to suggest further solutions for the improvement of these properties.

2.2.6. Validation of the docking method

This molecular docking method was validated for proving the reliability of the results. For this purpose, DockRMSD online program was used. This program can calculate RMSD value between two docked poses of a ligand and can render the result as text output [38]. For the validation of the docking method, co-ligand duroquinone was extracted from the protein file (pdb id:1dxo) then after adding the polar hydrogens and Gasteiger charges, docked again with the same protein. After this, docked and crystallographic poses of duroquinone were converted to convenient format (.pdbqt to .mol2) using Open Babel GUI [39]. In the end, these two files were submitted as input to DockRMSD online program.

3. Results

3.1. Chemistry

Synthesis of novel pyrrole-benzimidazoles **5a-n** outlined in Figure 1 begins with 4-chloro-benzenesulfonyl chloride as a starting material. Alkylation of the sulfonyl chlorides with iodoalkanes in the presence of tellurium, rongalite, and 1 M aqueous sodium hydroxide gave alkylsulfonyl derivatives (**1b**, **1c**) [18]. This was followed by reaction with conc. H₂SO₄ and potassium nitrate to give nitro compounds (**2a-c**) [18]. Aromatic nucleophilic substitution of the chlorine atom of 4-(alkylsulfonyl)-1-chloro-2-nitrobenzene (**2a-c**) with appropriated amines to provide the corresponding N-alkyl-4-(alkylsulfonyl)-2-nitroaniline derivatives **3a-n** in good yields [19,22]. Reduction of nitro group yielded to the crude amines **4a-n** [22] and these amines were used without purification. The resulting compounds (**5a-n**) were obtained by reacting o-phenylenediamines **4a-n** with pyrrole-2-carboxaldehyde in the presence of Na₂S₂O₅ and EtOH [22–24]. Yields were not optimized.

3.2. Biological activity

The in vitro effects of these novel pyrrole-benzimidazole derivatives on rat liver microsomal NADPH-dependent lipid peroxidation (LPO) levels and ethoxyresorufin O-deethylase (EROD) activity were monitored [9]. When compared to that observed for standard BHT, all synthesized compounds had moderate LPO inhibitory activity, particularly compounds **5b**, **5d**, and **5i-m** displayed high inhibitory activity on LPO with the inhibition rates of 77%–65%. However, none of these compounds had a marked inhibitory effect on EROD activity.

According to the comparison of substituents and activity results which are given in Table 1, we observe that when R₁ substituent is ethyl, the activity becomes elevated dramatically. Also, by using our R₁ ethyl-substituted compounds as a starting point, we can determine that nucleophilic groups such as benzyl at R₂ also would enhance the activity. Benzyl group needs to maintain electron density, therefore we encounter the decreasing values for compounds that are substituted with deactivating halogens: **5k**, **5l**, **5m**, and **5n**. If we examine **5b**, **5d**, and **5e** closely, R₁ is methyl and R₂ is ethyl. For **5d** (R₂ = butyl) and **5e** (R₂ = cyclohexyl), the lipid peroxidation inhibition slightly decreases. Moreover, the poor activity of compound **5n** can be explained by having propyl at R₁ and an electronically sparse aromatic ring at R₂. **5m** also has this aromatic portion at R₂ but has ethyl instead of propyl at R₁. This should possibly explain the relatively poor activity of **5n**. According to the LPO assay; compounds **5b**, **5d**, **5i**, **5j**, **5k**, **5l**, **5m** were elected as candidates. These compounds were compared to standard compound **BHT**. Among them, the most potent compound was **5j**.

3.3. Molecular docking and ADME studies

Initially, necessary positioning and interactions have been understood with the aid of a reference study, which mandates that the bound acceptor's aromatic moieties should become stacked with FAD and maintain certain interactions. Moreover, ligand should offer several interactions with aromatic residues such as Trp105, Phe106, Phe178, Tyr126, and Tyr128 and polar residue His161 [6]. Regarding Figure 2, compound **5j** docked into the binding site while maintaining hydrophobic interactions with Tyr128 through its benzyl substituent and benzimidazole moiety also constitutes Pi-alkyl interaction with Pro68. We can determine that the sulfonyl group acts as an acceptor in H-bond interactions with existing coenzyme FAD and Gly193.

The reliability of this method was proved using the DockRMSD distance calculation program. Out of 1,048,576 possible mappings, an optimal mapping was chosen by the same program. RMSD value for this mapping was calculated

Table 1. The inhibition values of synthesized pyrrole-benzimidazole derivatives **5a-n**, standards **BHT** and **Caffeine**, and control **DMSO** against EROD and LPO.

Chem no.	R ₁	R ₂	EROD (pmol/mg/min)	% of control	LPO (nmol/mg/min)	% of control
5a	-CH ₃	-CH ₃	44.25 ± 0.79	107	6.95 ± 1.76	43
5b	-CH ₃	-C ₂ H ₅	49.83 ± 0.09	120	4.83 ± 0.98	30
5c	-CH ₃	-C ₃ H ₇	44.90 ± 0.67	108	6.98 ± 0.66	43
5d	-CH ₃	-C ₄ H ₉	44.43 ± 1.29	107	5.61 ± 0.33	35
5e	-CH ₃	-cyclohexyl	24.83 ± 1.01	60	16.94 ± 2.75	104
5f	-CH ₃	-benzyl	44.17 ± 1.01	106	8.66 ± 1.33	53
5g	-CH ₃	-4-fluorobenzyl	44.64 ± 0.41	107	11.08 ± 0.19	68
5h	-CH ₃	-4-chlorobenzyl	45.37 ± 0.51	109	10.00 ± 0.99	62
5i	-C ₂ H ₅	-C ₃ H ₇	46.27 ± 1.22	111	5.07 ± 0.49	31
5j	-C ₂ H ₅	-benzyl	45.79 ± 0.19	110	3.73 ± 0.49	23
5k	-C ₂ H ₅	-p-fluorobenzyl	44.15 ± 0.75	106	5.37 ± 0.92	33
5l	-C ₂ H ₅	-3,4-difluorobenzyl	44.63 ± 0.21	107	5.11 ± 0.75	31
5m	-C ₂ H ₅	-3,4-dichlorobenzyl	44.83 ± 0.72	108	4.70 ± 0.29	29
5n	-C ₃ H ₇	-3,4-dichlorobenzyl	21.61 ± 2.00	52	15.51 ± 0.78	95
BHT			-		5.68 ± 0.22	35
Caffeine			6.41 ± 0.36	15	-	-
DMSO			41.53 ± 0.99	100	16.25 ± 1.45	100

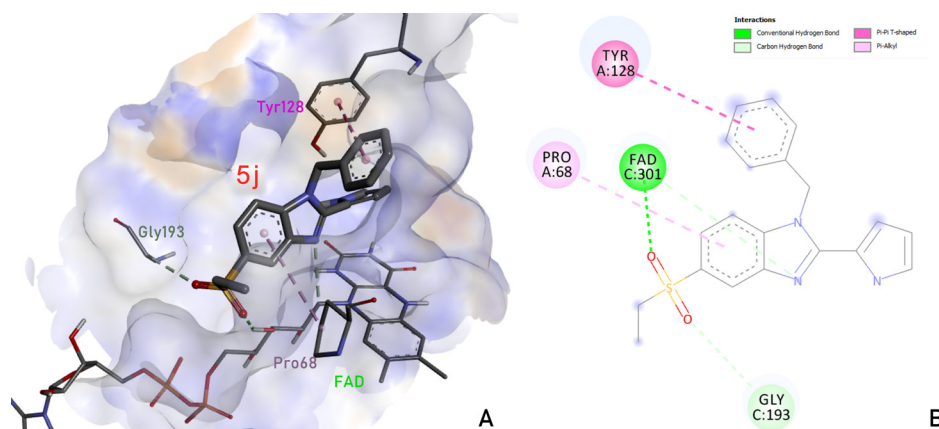


Figure 2. Binding pose (A) and ligand interaction diagram (B) of the most potent compound.

as 1.270 Å. For a reliable docking method, this value should be below 2 Å [40]. Fortunately, the RMSD value for these two duroquinone ligands was below this upper limit, therefore our method was proved to be rather versatile and reliable in conducting docking analysis with 1dxo.

The H-bond donor/acceptor count represents the atoms that are capable of interacting with the polar residues in the domains or cavities in the protein besides having an impact on P-glycoprotein transport, permeability, and many other parameters [36,41]. Number of rotatable bonds increases the overall flexibility of the compounds and give them the ability to interact with various enzymes and plasma proteins which have pharmacokinetic functions [36]. Using the Lipinski's rule of five (RO5) we can predict the oral activity of small molecules. This rule includes the following thresholds: the molecular mass should be below 500 daltons, calculated logP (clogP) must be less than 5.5, hydrogen bond donors should be less than or equal to 5 and hydrogen bond acceptors should be less than or equal to 10. Ligands that fail to conform to at least one of these parameters are flagged as orally undesirable [36,42,43]. Muegge's filter consists of the limits: $200 \leq$ molecular weight ≤ 600 , $-2 \leq$ XLOGP ≤ 5 , total polar surface area ≤ 150 , the number of rings ≤ 7 , the number of carbon > 4 , the number of heteroatoms > 1 , the number of rotatable bonds ≤ 15 , the hydrogen bond acceptors ≤ 10 , and the hydrogen bond donors ≤ 5 [44]. Leadlikeness is on the other hand, is a rule-based method that includes $250 \leq$ molecular weight ≤ 350 , XLOGP ≤ 3.5 , number of rotatable bonds ≤ 7 [36, 45].

Moreover, according to Table 2, compounds in our pyrrole-benzimidazole set have exhibited much better docking scores, interactions, and overall drug-likeness. Amongst these derivatives, docking scores for most effective LP inhibitors were found to be relatively lower than BHT and also other compounds. Additionally, the compounds **5g**, **5h**, **5l**, **5m**, and **5n** offered the lowest energy values and **5b**, **5d**, and **5i** passed all of the medicinal chemistry friendliness filters. Since the binding region consists of hydrophobic residues, H-bond acceptor/donor count has lost its relevance. One must note that all these parameters may affect the binding of drug-like compounds to proteins although a certain correlation is yet to be created. We have the knowledge that these ADME properties mainly have an impact on the bioavailability of substances.

The BOILED-Egg representation is a useful tool for the interpretation of permeation to the central nervous system (CNS) and gastrointestinal reabsorption. As result, all of the synthesized derivatives were found to be passively absorbable via the gastrointestinal tract. This finding increases the overall bioavailability of our compounds. Hereby we can determine that BHT can effectively pass through the blood-brain barrier (BBB) thus may cause mild CNS adverse effects. Besides, we can witness similar but milder hazards for the compounds except **5l**, **5m**, and **5n**. Among these, **5n** was found to have a much higher WLOGP (Figure 3). This may prevent the permeation of the compound through BBB thus having fewer adverse effects on CNS. These compounds have good absorption through the gastrointestinal tract while possessing a lower chance of permeating through BBB. Fortunately, they also exhibit high antioxidant activity. Overall, these attributes render these three compounds safe and versatile lead-like compounds.

4. Discussion

In this study, novel pyrrole-benzimidazole derivatives were designed, synthesized, and characterized and their antioxidant activities were then analyzed through lipid peroxidation and EROD activity. These derivatives exhibited moderate activities relative to BHT. Among all of them, compound **5j** emerged as a potential LPO inhibitor while having no considerable inhibitory effect against EROD activity. This characteristic may increase the chance of it being a potential agent against

Table 2. AutoDock Vina docking scores and SwissADME results of pyrrole-benzimidazole derivatives and BHT.

No.	Docking score (kcal/mol)	Interacting residues	Count of H-bond acceptors/donors	Number of rotatable bonds	Consensus computational LogP	Lipinski violations	Muegge Filter Violations	Leadlikeness
5a	-7.7	Tyr126 – H-bond Tyr126 – Pi-Pi Trp105 – Pi-Pi FAD – H-bond FAD – Pi-alkyl	4/1	2	0.92	0	0	Yes
5b	-8.0	Tyr128 – Pi-alkyl Tyr126 – Pi-Pi Trp105 – Pi-Pi His161 – Pi-alkyl FAD – H-bond FAD – Pi-Pi	4/1	3	1.20	0	0	Yes
5c	-8.1	Tyr126 – Pi-Pi Trp105 – Pi-Pi Phe178 – Pi-alkyl His161 – Pi-alkyl FAD – H-bond FAD – Pi-Pi FAD – Pi-alkyl	4/1	4	1.51	0	0	Yes
5d	-7.7	Gly149 – Carbon H-bond Tyr128 – Pi-Pi Tyr128 – Pi-alkyl Tyr126 – Pi-alkyl Gln66 – H-bond Pro68 – Pi-alkyl FAD – H-bond FAD – Carbon H-bond FAD – Pi-Pi	4/1	5	1.78	0	0	Yes
5e	-8.3	Tyr128 – Pi-Pi Tyr128 – Pi-alkyl Gly149 – Carbon H-bond Pro68 – Pi-alkyl FAD – H-bond FAD – Carbon H-bond FAD – Pi-Pi	4/1	3	2.13	0	0	Yes
5f	-8.6	Tyr128 – Pi-Pi Pro68 – Pi-alkyl FAD – H-bond FAD – Carbon H-bond FAD – Pi-Pi	4/1	4	2.07	0	0	No; MW>350
5g	-9.2	Tyr128 – Pi-Pi Tyr126 -Carbon H-bond Tyr126 – Pi-Pi Tyr126 – Pi-alkyl Phe178 – Pi-alkyl Trp105 – Pi-alkyl Glu123 – H-bond FAD – Pi-Pi FAD – Pi-alkyl	4/1	4	2.56	0	0	No; MW>350

Table 2. (Continued).

5h	-9.0	Tyr128 - Pi-Pi Tyr126 - Carbon H-bond Glu123 - H-bond Pro68 - Pi-alkyl FAD - Pi-Pi	5/1	4	2.37	0	0	No; MW>350
5i	-8.1	Tyr126 - Pi-Pi Trp105 - Pi-Pi Phe178 - Pi-alkyl His161 - Pi-alkyl FAD - Pi-Pi FAD - Pi-sigma	4/1	5	1.78	0	0	Yes
5j	-8.4	Tyr128 - Pi-Pi Gly193 - Carbon H-bond Pro68 - Pi-alkyl FAD - H-bond FAD - Carbon H-bond	4/1	5	2.35	0	0	No; MW>350
5k	-8.9	Tyr128 - Pi-Pi Tyr126 - Pi-donor H-bond Tyr126 - Pi-Pi Glu123 - H-bond Pro68 - Pi-alkyl FAD - Pi-Pi	5/1	5	2.64	0	0	No; MW>350
5l	-9.2	Tyr128 - Pi-Pi Tyr126 - Pi-donor H-bond Tyr126 - Pi-Pi Glu123 - H-bond Pro68 - Pi-alkyl FAD - Pi-Pi	6/1	5	2.93	0	0	No; MW>350
5m	-9.3	Tyr128 - Pi-Pi Tyr126 - Pi-donor H-bond Tyr126 - Pi-Pi Glu123 - H-bond FAD - Pi-Pi	4/1	5	3.31	0	0	No; MW>350, XLOGP3>3.5
5n	-9.4	Tyr128 - Pi-Pi Tyr126 - Pi-donor H-bond Tyr126 - Pi-Pi Glu123 - H-bond FAD - Pi-Pi	4/1	6	3.61	0	0	No; MW<250, XLOGP3>3.5
BHT	-6.0	Tyr128 - Pi-Pi Tyr128 - Pi-alkyl Tyr128 - Pi-sigma Tyr126 - Pi-alkyl Gly149 - Carbon H-bond FAD - Pi-sigma FAD - Pi-alkyl	1/1	2	4.24	0	2; XLOGP3>5, Heteroatoms<2	No; MW<250, XLOGP3>3.5

lipid peroxidation. SAR studies suggested that when R_1 becomes ethyl and R_2 is benzyl, the activity greatly enhances. Though when this benzyl group is substituted with the halogen group, activity is decreased.

Results of our studies suggest that pyrrole-benzimidazole derivatives have expressed much higher affinity values and a higher number of interactions in docking analysis, compared to that of standard BHT. Among them, compound **5j** which ensures certain interactions with the enzyme has shown promise as potential lipid peroxidation (LPO) inhibitor. This compound has offered hydrophobic interactions with Tyr128, a steric interaction with Pro68, and H-bond interactions with FAD and Gly193. Pharmacokinetic parameters were also calculated to discuss whether our compounds lack certain requirements for their pharmaceutical development or need certain improvements in this area. Among our derivatives, **5b** and **5d** have passed all the filters although other derivatives failed these requirements. These approaches have helped

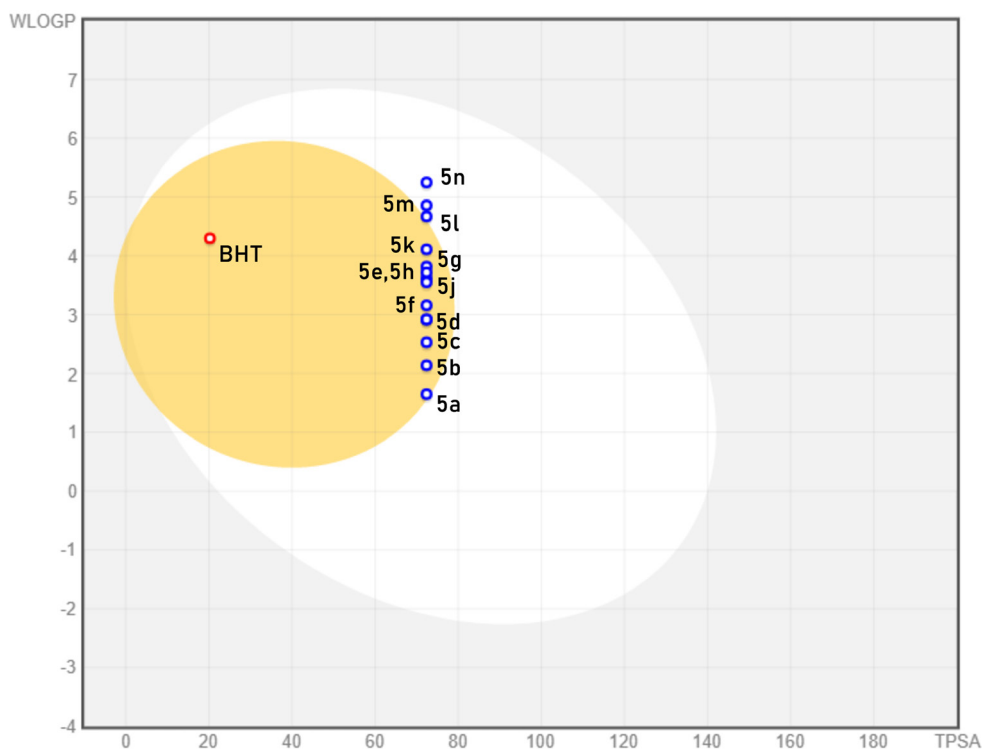


Figure 3. BOILED-Egg representation of pyrrole-benzimidazole derivatives and standard BHT. Compounds are represented as circles in this diagram. Circles that are located in the egg yolk area are predicted to passively permeate through the blood-brain barrier, and the white area covers the compounds which can be passively reabsorbed from the gastrointestinal tract. Red colour defines that the compound is not a substrate for P-glycoprotein while blue colour suggests the opposite. WLOGP and TPSA (topological polar surface area) are computational values that can be calculated in SwissADME.

our team to both discover a novel potent antioxidant agent and to gain a better understanding of certain drug-protein interactions which play a role in this particular activity.

Acknowledgment

The work was supported by Ankara University Research Grant under grant number: 16H0237010. Thanks to Mr. Greg Coleman who took time to check grammar and improve the clarity of the manuscript.

References

1. Ates-Alagoz Z, Can-Eke B, Coban T, Iscan M, Buyukbingol E. Antioxidant properties of novel benzimidazole retinoids. *Archiv der Pharmazie* 2004; 337: 188-192.
2. Birben E, Sahiner UM, Sackesen C, Erzurum S, Kalayci O. Oxidative stress and antioxidant defense. *World Allergy Organization Journal* 2012; 5 (1): 9-19.
3. Ramana KV, Ayala A, Muñoz MF, Argüelles S. Lipid peroxidation: production, metabolism, and signaling mechanisms of malondialdehyde and 4-hydroxy-2-nonenal. *Oxidative Medicine and Cellular Longevity* 2014; 360438.
4. Yin H, Libin X, Porter NA. Free radical lipid peroxidation: mechanisms and analysis. *Chemical Reviews* 2011; 111 (10): 5944–5972.
5. Pey AL, Megarity CF, Timson DJ. NAD(P)H quinone oxidoreductase (NQO1): an enzyme which needs just enough mobility, in just the right places. *Bioscience Reports* 2019; 39 (1): BSR20180459.
6. Faig M, Bianchet MA, Talalay P, Chen S, Winski S et al. Structures of recombinant human and mouse NAD(P)H:quinone oxidoreductases: species comparison and structural changes with substrate binding and release. *Proceedings of the National Academy of Sciences of the United States of America* 2000; 97 (7): 3177-3182.

7. Narule MN, Gaidhane MK, Gaidhane PK. Synthesis, characterization, biologically and antioxidant active of some 2-substitued 3,5-dimethyl-4-ethoxy carbonyl pyrrole derivatives. *Journal of Pharmacy Research* 2014; 6: 626-632.
8. Shanty AA, Philip JE, Sneha EJ, Prathapachandra Kurup MR, Balachandran S et al. Synthesis, characterization and biological studies of Schiff bases derived from heterocyclic moiety. *Bioorganic Chemistry* 2017; 70: 67-73.
9. Kerimov I, Kilcigil G, Özdamar ED, Eke B, Çoban T et al. Design, one pot and microwave assisted synthesis of 2-amino/5-aryl-1,3,4-oxadiazoles bearing benzimidazole moiety as antioxidant. *Archiv der Pharmazie* 2012; 345 (7): 549-556.
10. Kilcigil G, Alp AS, Coban T, Ozdamar ED, Eke B. Synthesis and evaluation of antioxidant properties of novel 2-[2-(4-chlorophenyl)benzimidazole-1-yl]-N-(2-arylmethylene amino) acetamides and 2-[2-(4-chlorophenyl)benzimidazole-1-yl]-N-(4-oxo-2-arylthiazolidine-3-yl) acetamides-I. *Chemical Biology & Drug Design* 2012; 76: 869-877.
11. Ayhan-Kilcigil G, Kus C, Coban T, Ozdamar ED, Can-Eke B. Identification of a novel series of N-Phenyl-5-[(2-phenylbenzimidazol-1-yl)methyl]-1,3,4-oxadiazol-2-amines as potent antioxidants and radical scavengers. *Archiv der Pharmazie* 2014; 347 (4): 276-282.
12. Alp AS, Kilcigil G, Ozdamar ED, Eke B. Synthesis and evaluation of antioxidant activities of novel 1,3,4-oxadiazole and imine containing 1H-benzimidazoles. *Turkish Journal of Chemistry* 2015; 39: 42-53.
13. Iscan MY, Buyukbingol E, Iscan M, Sahin F, Safak C. Effects of 2-arylbenzimidazoles on rat hepatic microsomal monooxygenase system. *Comparative Biochemistry and Physiology* 1989; 92C: 109-115.
14. Little PJ, Ryan AJ. Inhibitors of hepatic mixed function oxidases. 4. Effects of benzimidazole and related compounds on aryl hydrocarbon hydroxylase activity from phenobarbitone and 3-methylcholanthrene induced rats. *Journal of Medicinal Chemistry* 1982; 25: 622-626.
15. Dickens M, Bridges JW. The relationship between the binding of 2-n-alkylbenzimidazoles to rat hepatic microsomal cytochrome P-450 and the inhibition of monooxygenation. *Biochemical Pharmacology* 1982; 31: 1315-1320.
16. Murray M, Ryan AJ. The binding to oxidized cytochromes P-450 and inhibition of mixed-function oxidases by aryl-substituted benzimidazoles and related compounds. *Chemico-Biological Interactions* 1983; 43: 341-351.
17. Ates-Alagoz Z. Antioxidant activities of retinoidal benzimidazole or indole derivatives in *in vitro* model systems, *Current Medicinal Chemistry, Special Issue "Chemistry and Biology of Antioxidants"* 2013; 20 (36): 4633-4639.
18. Ates Z, Can-Eke B, Suzen S, Iscan M, Buyukbingol E. Effects of a benzimidazole compound on monooxygenase activities. *Farmaco* 1997; 52: 703-706.
19. Ates-Alagoz Z, Kus C, Coban T. Synthesis and antioxidant properties of some novel benzimidazoles containing substituted indole or 1,1,4,4-tetramethyl-1,2,3,4-tetrahydro-naphthalene fragments. *Journal of Enzyme Inhibition and Medicinal Chemistry* 2005; 20 (4): 325-331.
20. Ates-Alagoz Z, Coleman N, Martin M, Wan A, Adejare A. In vitro anticancer properties of novel radiosensitizer analogs. *Chem Biol & Drug Design* 2012; 80: 853-861.
21. Shavnya A, Hesp KD, Mascitti V, Smith AC. Palladium-catalyzed synthesis of (hetero)aryl alkyl sulfones from (hetero)aryl boronic acids, unactivated alkyl halides, and potassium metabisulfite. *Angewandte Chemie International Edition* 2015; 54: 13571-13575.
22. Goker H, Alp M, Ates-Alagoz Z, Yıldız S. Synthesis and potent antifungal activity against *Candida* species of some novel 1H-benzimidazoles, *Journal of Heterocyclic Chemistry*. 2009; 46 (5): 936-948.
23. Zengin-Karadayı F, Yaman M, Kışla MM, Keskus AG, Konu O et al. Design, synthesis and anticancer/antiestrogenic activities of novel indole-benzimidazoles. *Bioorganic Chemistry* 2020; 100.
24. Zengin-Karadayı F, Yaman M, Kışla MM, Konu O, Ates-Alagoz Z. Design, synthesis, anticancer activity, molecular docking and ADME studies of novel methylsulfonyl indole-benzimidazoles in comparison with ethylsulfonyl counterparts. *New Journal of Chemistry* 2021; 45 (20): 9010-9019.
25. Lowry OH, Rosebrough NJ, Farr AL, Randall RJJ. Protein measurement with the Folin phenol reagent. *Journal of Biological Chemistry* 1951; 193 (1): 265-275.
26. Wills ED. Mechanisms of lipid peroxide formation in animal tissues. *Biochemical Journal* 1966; 99: 667-676.
27. Wills ED. Lipid peroxide formation in microsomes. General considerations. *Biochemical Journal* 1969; 113: 333-341.
28. Bishayee S, Balasubramanian AS. Lipid peroxide formation in rat brain. *Journal of Neurochemistry* 1971; 18: 909-920.
29. Iscan M, Arinc E, Vural N, Iscan MY. In vivo effects of 3-methylcholanthrene, phenobarbital, pyrethrum and 2,4,5-T isooctylester on liver, lung and kidney microsomal mixed-function oxidase system of guinea-pig: a comparative study. *Comparative Biochemistry and Physiology* 1984; 77C: 177-190.
30. Burke MD, Thompson S, Elcombe CR, Halpert J, Haaparanta T et al. Ethoxy, pentoxy- and benzyloxyphenoxazones and homologues: a series of substrates to distinguish between different induced cytochromes P-450. *Biochemical Pharmacology* 1985; 34: 3337-3345.

31. Berman HM, Westbrook J, Feng Z, Gilliland G, Bhat TN et al. The Protein Data Bank. *Nucleic Acids Research* 2000; 28: 235-242.
32. Morris GM, Huey R, Lindstrom W, Sanner MF, Belew RK et al. Autodock4 and AutoDockTools4: automated docking with selective receptor flexibility. *Journal of Computational Chemistry* 2009; 16: 2785-2791.
33. Hanwell MD, Curtis DE, Lonie DC, Vandermeersch T, Zurek E et al. Avogadro: An advanced semantic chemical editor, visualization, and analysis platform. *Journal of Cheminformatics* 2012; 4: 17.
34. Trott O, Olson AJ. AutoDock Vina: improving the speed and accuracy of docking with a new scoring function, efficient optimization and multithreading. *Journal of Computational Chemistry* 2010; 31: 455-461.
35. Dassault Systèmes BIOVIA, Discovery Studio Visualizer v17.2.0.16349, San Diego: Dassault Systèmes 2017.
36. Daina A, Zoete V. SwissADME: a free web tool to evaluate pharmacokinetics, drug-likeness and medicinal chemistry friendliness of small molecules. *Nature: Scientific Reports* 2017; 7 (1): 42717.
37. Daina A, Zoete V. A BOILED-Egg to predict gastrointestinal absorption and brain penetration of small molecules. *ChemMedChem* 2016; 11 (11): 1117-1121.
38. Bell EW, Zhang Y. DockRMSD: an open-source tool for atom mapping and RMSD calculation of symmetric molecules through graph isomorphism. *Journal of Cheminformatics* 2019; 11: 40.
39. O'Boyle NM, Banck M, James CA, Morley C, Vandermeersch T, Hutchison GR. OpenBabel: An open chemical toolbox. *Journal of Cheminformatics* 2011; 3: 33.
40. Castro-Alvarez A, Costa AM, Vilarrasa J. The performance of several docking programs at reproducing protein-macrolide-like crystal structures. *Molecules* 2017; 22 (1): 136.
41. Desai PV, Raub TJ, Blanco MJ. How hydrogen bonds impact P-glycoprotein transport and permeability. *Bioorganic & Medicinal Chemistry Letters* 2012; 22 (21): 6540-8.
42. Mullard A. Re-assessing the rule of 5, two decades on. *Nature Reviews Drug Discovery* 2018; 17: 777.
43. Lipinski CA, Lombardo F, Dominy BW, Feeney PJ. Experimental and computational approaches to estimate solubility and permeability in drug discovery and development settings. *Advanced Drug Delivery Reviews* 2001; 46 (1-3): 3-26.
44. Muegge I, Heald SL, Brittelli D. Simple selection criteria for drug-like chemical matter. *Journal of Medicinal Chemistry* 2001; 44 (12): 1841-6.
45. Teague S, Davis A, Leeson P, Oprea, T. The design of leadlike combinatorial libraries. *Angewandte Chemie International Edition England* 1999; 38: 3743-3748.